

OMAE2018-77959

## COMPARISON OF FUEL CONSUMPTION ON A HYBRID MARINE POWER PLANT WITH LOW-POWER VERSUS HIGH-POWER ENGINES

### Zhenying Wu

Norwegian University of Science  
and Technology (NTNU)  
Department of Marine Technology  
7491 Trondheim, Norway  
Email: zhenyingwu@hotmail.com

### Laxminarayan Thorat\*

Norwegian University of Science  
and Technology (NTNU)  
Department of Marine Technology  
7491 Trondheim, Norway  
Email: laxminarayan.thorat@ntnu.no

### Roger Skjetne

Norwegian University of Science  
and Technology (NTNU)  
Centre for Autonomous Marine  
Operations and Systems (AMOS)  
Department of Marine Technology  
7491 Trondheim, Norway  
Email: roger.skjetne@ntnu.no

### ABSTRACT

*In this paper, we are comparing fuel consumption on a case study hybrid marine power plant with diesel gensets and batteries. Optimization methods are used to find an optimal operating point for the gensets, under different power demands, with regards to fuel consumption and  $NO_x$  emissions. Three different power system example configurations for an offshore construction vessel are explored in this study, and the simulations are carried out to compare the resulting fuel consumption and  $NO_x$  emissions for these power system configurations.*

### Nomenclature

DP	Dynamic positioning
ESS	Energy storage system
FC	Fuel consumption
Genset	Generator set
MCR	Maximum continuous rating
OCV	Offshore construction vessel
ROV	Remote operated vehicle
SFC	Specific fuel consumption

### INTRODUCTION

In the last century, diesel-electric propulsion systems have been installed on many vessels such as supply vessels, drilling ships, icebreakers, and other offshore installations. In diesel-electric propulsion systems, the engine is first connected to a generator that supplies a power distribution network and drives the electric motors. Electric propulsion has become a prevailing trend mainly due to increased demands for energy-efficient and low emission vessels with high availability and reliability. A vessel with diesel-electric propulsion often has between 2 to 10 pairs of diesel engines and generators. The gensets can be started and stopped as required in a configuration where there are more than two gensets, while at the same time keeping redundancy [1, 2].

Due to operation cost and environmental concerns, there is ongoing effort to reduce the fuel consumption and emissions in all transportation sectors including marine transportation [3]. It is usually desired to operate the engine at a loading rate between 60% and 80% to achieve the lowest fuel consumption per kilowatt produced. However, operating condition can vary a lot so that the engines are not always operated within such load range. When there exist varying load conditions, configuring the power system with many low-power marine engine sets is beneficial, due to the fact that higher loading percentage per engine can then be achieved by shutting down unnecessary ones while at the same time keeping redundancy.

---

\* Address all correspondence to this author.

There are many benefits to install a modern hybrid diesel-electric propulsion system with energy storage capacity instead of a traditional diesel-electric system. Using energy storage systems (ESS) in marine vessels is a new practice, and new rules regulating ESS onboard ships have recently been published by DNV GL [4]. During operations of offshore installation vessels, there is a large range of average loading between 10% to 90%, and this is also accompanied by fast varying load transients. Integrating ESS in the power system can achieve higher flexibility and more degrees of freedom to optimize the operation of the diesel engines. Combining gensets with ESS have shown through different usage strategies to have a potential for improving the fuel economy as well as enhancing the genset dynamics to reduce fuel consumption, emissions, wear and tear, and maintenance cost [5, 6].

Even if the investment cost is higher for a diesel-electric system with ESS, it will often pay off in the end as it leads to less operating cost. However, not all ships will benefit equally from this system configuration, and the advantages will to a large extent be determined by the static and dynamic power requirements related to the vessel's operating profile.

### Genset Sizing

The ships can have different types of engines from 2- or 4-stroke diesel engines to turbines or just several gensets that power thrusters or pods. The selection of components for the marine power plant mainly depends on the type of operations for which the ship is designed.

Power capacity (sizing) of gensets may have an important effect on power efficiency. A genset of high capacity typically has a better fuel efficiency and emission footprint at the optimal loading condition. However, its fuel efficiency will in practice often be low since the load per genset when operating in nice weather with small environmental loads is typically far from the optimal 60-80% loading, especially when redundancy requirements on online spinning reserve demands more online gensets than the loading conditions imply. From a fuel efficiency point of view, many smaller gensets may then be more beneficial, since then it is easier to determine an online configuration of gensets that ensures both optimal loading and redundancy to failure [7].

On the other hand, the optimal sizing of the gensets will depend on a vessel's operational profile and weather condition in the operational area. Generally, a vessel has a typical operational profile that represents the likely conditions the vessel will encounter and for how long, based on the intended use of the vessel. However, often the actual use of the vessel changes from its originally planned operating profile - e.g. due to market conditions, and then the ship owner is stuck with an inefficient power plant configuration for this new operating regime. Again, a hybrid power plant with more smaller capacity gensets offer a greater flexibility to reconfigure the power plant according to

new operating conditions.

In conventional engine design, the reason to increase the number of cylinders is to increase the torque and power with the improved balancing of forces and momentum. These properties become less important in a diesel-electric propulsion design. Less number of cylinders lead to simpler maintenance and higher robustness, thereby increasing the availability.

In this study, low- and high-power engines that have the same cylinder characteristics but different cylinder numbers are considered. Due to the variations in manufacturing techniques and designs, it is hard to compare small and large engines in a wide range. Hence, low-power engines refer to engines with one or several cylinders while high-power engines have more piston cylinder pairs.

### Genetic Algorithm for Optimization

A genetic algorithm (GA) is an optimization method based on a natural selection process that mimics biological evolution. It consists of a population of bit strings processed by three genetic operators, which are selection, crossover, and mutation. Each string represents a possible solution for the problem being optimized, and each bit represents a value for a variable of the problem. To classify the solution of a given bit string, a fitness function must be established. Besides, other criteria can be set in addition to achieving the desired optimum [8].

The advantage of GA is its use of stochastic operators instead of deterministic rules to search for fitness solutions. The search process jumps randomly from point to point, thus allowing escape from a local optimum, in which other conventional optimization algorithms might land. Therefore, GA is a promising method to solve complex, multi-variable optimization problems. On the other hand, the main drawback of GA is that it gives no guarantee of finding the global optimum, and it is less suited than other optimization methods for real-time computation.

In this study, we use the GA method to find an optimal operating point for the gensets, under different power demands, with regard to fuel consumption and NO<sub>x</sub> emission. Three power system configurations for an offshore construction vessel are explored in this study:

1. Marine power plant with large capacity gensets.
2. Marine power plant with small capacity gensets of the same cylinder characteristic as in 1.
3. Marine power plant with small capacity gensets of different cylinder characteristic.

Mathematical formulations are developed for both single and multiple objective optimization studies of direct current (DC) hybrid marine power system at static load, where the optimization objective is to minimize the fuel consumption and NO<sub>x</sub> emission. For a given power demand, the variables in the optimization problem are the engine speed, torque, and the connect sta-

tus (on/off) with certain constraints. Typical power demand is a stepwise profile from 3% to 100% of the total installed power capacity.

The GA method has been applied to solve most of the optimization problems, while an ESS usage method proposed by [6] has been used and compared with the GA method in a case study where the total fuel consumption during an operation is optimized via optimal charging and discharging of an ESS. In order to reduce the computational burden and time while ensuring optimization quality, Monte Carlo simulations are applied to optimization results for verification.

The contributions of this paper are an optimization formulation, a fuel consumption and NO<sub>x</sub> emission analysis of a case study, and a comparison of results of the configurations with low-power versus high-power engines.

The mentioned tasks and analysis are mainly limited to designs for offshore construction vessels. Other types of vessel are not in the scope of this research, due to different load profiles and power management requirements. The optimization study is based on static power requirement, and the extra fuel consumption and emission caused by power transients and engine start/stop are not considered. The ESS usage strategies in this study are mainly start-and-stop and strategic loading [6], as the focus is not placed on load transients. Besides, the results from this study are case-specific, due to the assumption of certain operational profile, load power requirements and specific engine SFC maps.

## VESSEL CONFIGURATION

The OCV is capable of performing subsea construction and equipment installation as well as inspection, maintenance, and ROV services. Important features of such vessels are sufficient stability that allows station-keeping and roll damping, and good sea-keeping performance that provides a safe platform for crew and cargo during operation. It has high demands on the flexibility, efficiency, and reliability, and thus it is beneficial to have a DC grid hybrid power system. Therefore, the OCV is chosen in this case study.

### Vessel Load and Power System Specification

The offshore construction vessel in this study is equipped with two main propellers ( $2 \times 3000 \text{ kW}$ ), two bow thrusters ( $2 \times 1335 \text{ kW}$ ), and two azimuth thrusters ( $2 \times 850 \text{ kW}$ ). Other loads such as lifting and ventilation are considered to be up to  $60 \text{ kW}$ . Therefore, the maximum total load is  $10.43 \text{ MW}$ .

The propulsion system ensures the redundancy as what is required by DP2, that is, the loss of position does not occur in the event of a single failure in active components as specified in Sec.2.6.1 [4]. A DP2 or DP3 system guarantees high uptime to both FPSO and production platforms, for twenty-four hours a

**TABLE 1.** ENGINE CHARACTERISTICS [9, 10]

	Minimum SFC	Maximum SFC
	$g/kW \cdot h$	$g/kW \cdot h$
RR Bergen B32:40V12A	180	250
RR Bergen B32:40L3	180	250
Perkins 2506C	205	245

day, under challenging conditions. In this study, the requirement of at least 2 engines for DP2/DP3 is made aware of, and this could easily be included. However, we did not want to complicate the study with this requirement, in order to assess optimality also with very small loads and only one engine running.

The MCR of the power system can be calculated based on the total load and typical efficiency from these loads to the diesel engine shaft. The efficiency from thruster loads and other loads to the engine shaft is assumed to be 90%, taking the efficiencies of the motor, frequency converter, rectifier, and generator into account. Hence, the maximum loading of the diesel engines is  $10.43/0.9 = 11.59 \text{ MW}$ .

This could be provided by two or more engines. It should be noted that a realistic design will typically choose to use 4-6 engine sets to enhance the general performance of the vessel while optimizing the total cost. In our case, we are interested in comparing the configuration with large power-rating engines and medium-small power-rating engines. On the other hand, there is a limited accessible data for fuel consumption and NO<sub>x</sub> emission mapping of the engines. Based on the data we have found, we have therefore developed the following configurations:

1. Two medium speed engines (Rolls Royce (RR) Bergen B32:40V12A) with ESS.
2. Eight medium speed engines (RR Bergen B32:40L3) with ESS.
3. Thirty medium speed engines (Perkins 2506C) with ESS.

The characteristics of the engines involved in this study are summed up in Table 1. It is clear that both Bergen engines have better overall fuel efficiency than the Perkins 2506C engine, so that the optimal specific fuel consumption in configuration 3 is 12.2% higher than in the other two configurations. It should be noted that all engines are 4-stroke diesel engines. We do not propose these as actual configurations for this vessel, but use them as cases to study FC and NO<sub>x</sub> emission with respect to small, medium, and large capacity configurations. An actual optimal power plant design should likely be a mix of these.

## OPTIMIZATION PROBLEM FORMULATION

Due to DC distribution in all configurations, individual engine speed and torque can be adapted to achieve optimal performance in regard to fuel consumption and/or NO<sub>x</sub> emission at a certain load. Moreover, as a result of multiple gensets, engines can be started or shut down so that the remaining online engines can run optimally. Therefore, for each engine there are three variables to optimize, being engine speed, engine torque, and engine status (on/off). For a total of  $m$  engines, these optimization variables are denoted by the vectors

$$\omega_i = [\omega_1, \omega_2, \dots, \omega_m] \quad (1)$$

$$T_i = [T_1, T_2, \dots, T_m] \quad (2)$$

$$s_i = [s_1, s_2, \dots, s_m] \quad (3)$$

where  $\omega_i$  denotes speed,  $T_i$  denotes torque, and  $s_i$  denotes status of engine  $i$ , respectively. The engine speed and engine torque are continuous variables in the operational region of an engine, while the running status is a discrete variable which is limited to be 0 (off) or 1 (on).

### Steady State Engine Map

The energy production efficiency of a diesel engine are typically expressed by SFC, calculated by

$$\text{SFC} = \frac{FC}{P} \quad (4)$$

$$P = T \cdot \omega, \quad (5)$$

where  $FC$  is the fuel consumption rate in grams per second;  $P$  is the engine power produced in kilowatts. Similarly, the specific NO<sub>x</sub> emission is calculated by

$$\text{SNO}_x = \frac{\text{NO}_x}{P}. \quad (6)$$

The SFC and SNO<sub>x</sub> emission generally depends on many variables such as engine mean effective pressure, engine angular speed, engine power, etc. An engine's SFC and SNO<sub>x</sub> curves against cylinder power and speed are generally obtained by running experiments at different operating points. In this study, the applied engine SFC and SNO<sub>x</sub> maps are by courtesy of the Hybrid Power Lab at NTNU, Trondheim, as a resource from [11]. Linear interpolation is used on these maps to find optimum operating points. The maps are given in the appendix .

### Single Objective Optimization Problem Formulation

From the above information, the optimization problem to minimize fuel consumption can be formulated mathematically

by

$$\begin{aligned} \min_{\omega, T, s} \quad & F(\omega, T, s) = \sum_{i=1}^m s_i \cdot \omega_i \cdot T_i \cdot \text{SFC}(\omega_i, T_i) \\ \text{s.t.} \quad & P_L \leq \sum_{i=1}^m s_i \cdot \omega_i \cdot T_i \leq P_H \\ & T_i \leq a \cdot \omega_i + b, \quad i = 1, \dots, m \\ & T_{i,\min} \leq T_i \leq T_{i,\max} \\ & \omega_{i,\min} \leq \omega_i \leq \omega_{i,\max} \\ & s_i \in \{0, 1\} \end{aligned} \quad (7)$$

where we will describe the parameters later. Similarly, we formulate the NO<sub>x</sub> optimization by

$$\begin{aligned} \min_{\omega, T, s} \quad & N(\omega, T, s) = \sum_{i=1}^m s_i \cdot \omega_i \cdot T_i \cdot \text{SNO}_x(\omega_i, T_i) \\ \text{s.t.} \quad & P_L \leq \sum_{i=1}^m s_i \cdot \omega_i \cdot T_i \leq P_H \\ & T_i \leq a \cdot \omega_i + b, \quad i = 1, \dots, m \\ & T_{i,\min} \leq T_i \leq T_{i,\max} \\ & \omega_{i,\min} \leq \omega_i \leq \omega_{i,\max} \\ & s_i \in \{0, 1\} \end{aligned} \quad (8)$$

### Multi-Objective Optimization Problem

From the above information, the final formulation of the optimization problem can be mathematically represented by

$$\begin{aligned} \min_{\omega, T, s} \quad & [F(\omega, T, s), N(\omega, T, s)] \\ \text{s.t.} \quad & P_L \leq \sum_{i=1}^m s_i \cdot \omega_i \cdot T_i \leq P_H \\ & T_i \leq a \cdot \omega_i + b, \quad i = 1, \dots, m \\ & T_{i,\min} \leq T_i \leq T_{i,\max} \\ & \omega_{i,\min} \leq \omega_i \leq \omega_{i,\max} \\ & s_i \in \{0, 1\} \end{aligned}$$

This is a general multi-objective optimization problem, and weights can be selected and applied to the objective function in a more specific case.

### Constraints

The constraints in this problem are mainly on the power demand, that is, the power produced by all engines should be equivalent to the power required from load. In a strict way, this power

**TABLE 2.** SIMULATION SETTING FOR OPTIMIZATION OF FC AT STATIC LOAD

	Variables	Population size	Iterations	Function tolerance
Config. 1	4	50	100	$10^{-3}$
Config. 2	24	100	150	$10^{-5}$
Config. 3	90	200	200	$10^{-5}$

constraint is an equality constraint. In practice, however, we can regard this as an inequality constraint to account for some power demand fluctuations, as well as letting an ESS can supply the power difference. Therefore, the power constraint can be set between a high power demand  $P_H$  and low power demand  $P_L$  for each load setpoint. It should be noted that the differences between  $P$  and  $P_L$ ,  $P_H$  should not exceed the charging/discharging capacity of the ESS. Another constraint is due to the limited operating area of each engine. That is to say, an engine can only produce a limited range of power for a given speed, and a higher power demand may require a higher speed. Besides,  $a$  and  $b$  are indexes which are obtained from the engine SFC map; while  $\omega_{i,min}$ ,  $\omega_{i,max}$ , and  $T_{i,min}$ ,  $T_{i,max}$  are lower and upper limits on speed and torque within which the engine operates.

## CASE STUDY

All the simulations have been carried out using MATLAB. The average computation time for a single objective optimization problem is around 100 seconds, and around 3000 seconds for the multi-objective optimization problem.

### Fuel Consumption at Static Load

The first case is a single objective optimization problem when the gensets operate at static load demand, which are loads from 3%, 6%, 10%, 15%, and 20% to 100% MCR with an interval of 10%. The reason for a denser interval in low-power setting is that many OCVs experienced a fuel-consumption problem in that range. The simulation setting is shown in Table 2. The results from the simulations are shown in Figures 1, 2, and 3. At low loading rate upto 15%, the configuration consists of 30 Perkins gensets (configuration 3) has slightly better performance in fuel consumption than the configuration that consists of 2 higher power-rating Bergen gensets (configuration 1). The fuel consumption resulted from 8 low power-rating Bergen gensets (configuration 2) is lower than in the other two configurations by approximately 50 000 g/h. At low loading, the online gensets in configuration 3 have percentage loading higher than the optimal loading and the online gensets in configuration 1 have low loading resulting in higher fuel consumption.

As the static load increases, the fuel consumption increases

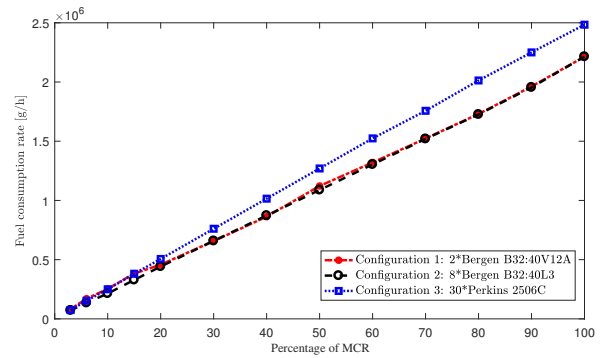


**FIGURE 1.** FUEL CONSUMPTION AT STATIC LOAD

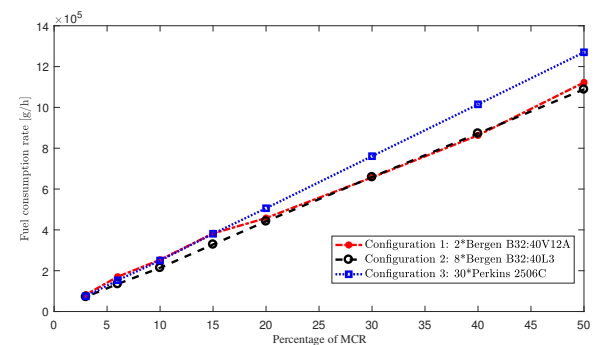


**FIGURE 2.** ZOOM VIEW OF FIGURE 1

faster for configuration 3 than for the other two configurations. At static load around 15% MCR, configuration 1 and 3 have almost equal fuel consumption. After this point, the performance of configuration 3 deteriorates and ends up with a larger fuel consumption of around 300 000 g/h compared to configurations 1 and 2 at 100% MCR. This makes sense since the optimal SFC of Perkins genset is 25 g/kWh higher than the other two Bergen gensets, which is 12.2% percent higher than its optimum. Thus, the Perkins diesels have their main advantage at low loading conditions due to their smaller capacity. On the other hand, as the two different Bergen engines have the same fuel consumption characteristics and the only difference is their cylinder number, the fuel consumption at high load for these two configurations are almost the same. However, with the improved ability to stop unnecessary engines, configuration 2 outperforms configuration 1 at loads lower than 50% of the maximum installed capacity.

Figure 3 illustrates the number of running engines in different configurations. It is clear that both engines in the configuration 1 must work at the mid-high load range, while single engine work at low load range. For the configurations 2 and 3, the number of online engines increases fast up to approximately 60% and then flattens out. The reason for this is that fewer engines sharing

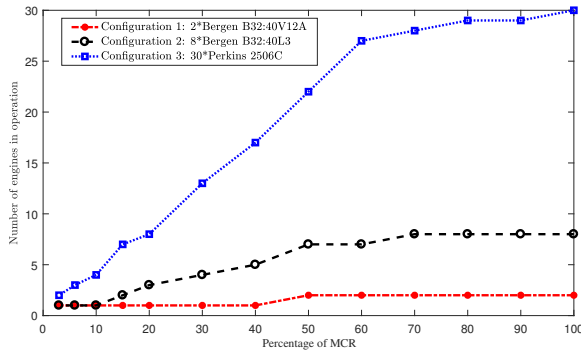


FIGURE 3. ONLINE ENGINES AT STATIC LOAD.

the same load lead to more optimal operating condition for every single engine and hence reduced fuel consumption.

### Efficiency Degradation

The power efficiency of the generator is usually considered to be around 96%, where power efficiency is defined to be its output power dividing by its input power. However from engine shaft to load, there exists transmission losses. The power loss is typically assumed to be negligible when it comes to the switch-board, while power efficiency of the power converter is assumed to be around 98%-99.5%. Meanwhile, the power efficiency of the electric motor is around 96%. However, all these values are specified on the product's data sheet at rated condition by manufacturers. As a result, power supply efficiency is usually specified based on the operating conditions that are most favourable to the figure concerned, for example, at maximum rated load. However, for the rest of the time, it will be operating below full load, and efficiency is likely to be much lower.

In this simulation study, we modified the engine power in the constraints to include converter efficiency degradation. The converter efficiency curve is shown in Figure 4. The set up of simulation is the same as what has shown in Table 2. The results is displayed in Table 3 and Figure 5. The total shape and trend of the curves in Figure 5 is very similar as in Figure 1. However, we observe some differences if we take a close look at low to middle load. At 10% MCR, configuration 1 used to have higher (approximately 16.6%) fuel consumption than configuration 3. The situation changes when converter efficiency degrading is considered, where fuel consumption in configuration 3 is around 6% less than in configuration 1. The cross-point where fuel consumption in configuration 1 and 2 approximately equals used to be 60% MCR without considering converter efficiency change, which now increases to 80%. This indicates the advantage that high-power engines have at high load is weakened when efficiency degradation is taken into account. Comparing before and after considering  $\eta_c$ , fuel consumption increased at highest

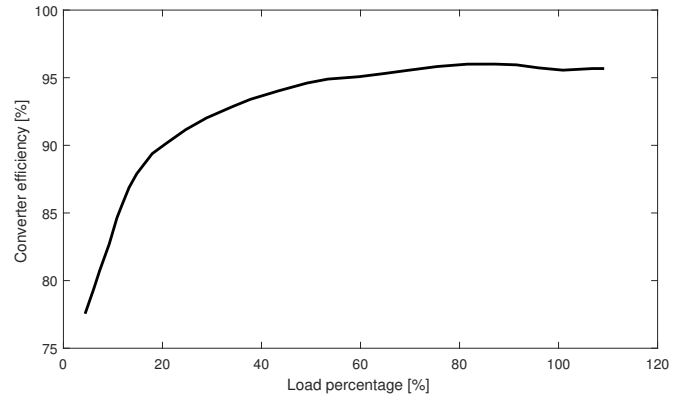
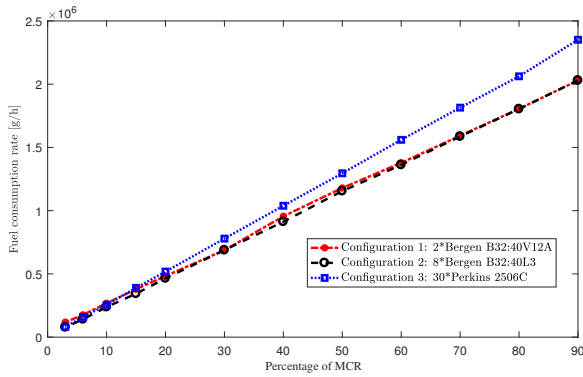


FIGURE 4. CONVERTER EFFICIENCY AGAINST LOAD PERCENTAGE [12]

TABLE 3. FUEL CONSUMPTION COMPARISON (in kg/h) BEFORE AND AFTER INCLUDING  $\eta_c$

Load	Config. 1		Config.2		Config. 3	
	w/o $\eta_c$	w $\eta_c$	w/o $\eta_c$	w $\eta_c$	w/o $\eta_c$	w $\eta_c$
3%	83	119	72	79	74	82
6%	170	176	135	141	153	160
10%	253	268	214	238	250	256
15%	383	392	329	343	381	389
20%	490	507	442	465	506	518
30%	706	735	659	688	761	779
40%	901	955	872	913	1015	1038
50%	1122	1179	1088	1155	1270	1295
60%	1320	1378	1304	1362	1524	1560
70%	1523	1593	1520	1586	1727	1814
80%	1730	1805	1726	1803	2013	2062
90%	1955	2030	1955	2030	2250	2351

30% in configuration 1, 10% in configuration 2 and only 2.3% in configuration 3; Besides, fuel consumption increased 4.2%, 4.3% and 2.4% in configuration 1, 2, and 3 respectively when delivering 80% MCR power. Comparing Figure 6 with Figure 3, one can tell that the number of the engines in operation in configuration 1 and 2 are exactly the same. However, the number of running engines in configuration 3 increases, particularly at low load. For example, the engine number increased from 8 to 9 at 20% MCR. This may be caused by more optimal fuel efficiency to start another engine when engine load increases by a small step.



**FIGURE 5.** FUEL CONSUMPTION OF 3 CONFIGURATIONS AT STATIC LOAD (CONSIDERING EFFICIENCY DEGRADATION).

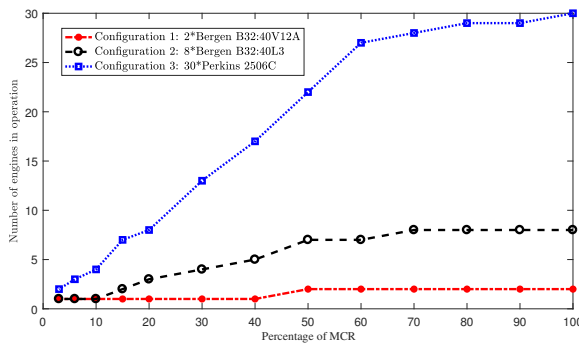


**FIGURE 6.** ONLINE ENGINES AT STATIC LOAD (CONSIDERING EFFICIENCY DEGRADATION).

**TABLE 4.** SIMULATION SETTING FOR MULTI-OBJECTIVE OPTIMIZATION

	Variables	Population size	Iterations	Function tolerance
Config. 3	90	200	200	$10^{-5}$

### Multi-Objective Optimization

The multi-objective optimization was carried out for configuration 3 at 3 different load conditions (10%, 20% and 50% MCR). The setting of this simulation is indicated in Table 4. A typical offshore construction vessel operates at load lower than 60% MCR during around 80% of its operating time [11]. Therefore, we chose three load points to study in multi-objective optimization, which are 10%, 20% and 50%. Figure 7 depicts the resulting pareto front in this case, and it provides possible optimal candidates, which can be chosen according to different criteria.

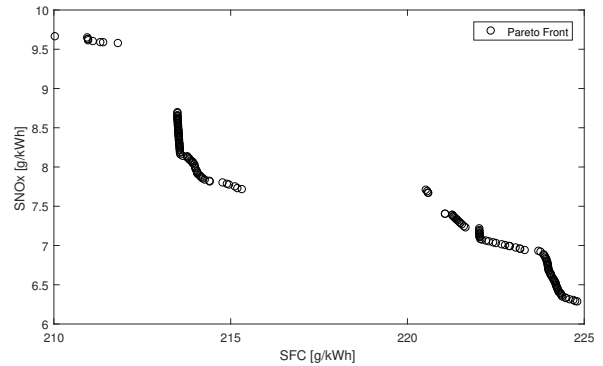


**FIGURE 7.** MULTI-OBJECTIVE OPTIMIZATION RESULT AT 10% MCR

The fuel consumption at 10% load only minimizing specific fuel consumption is 210 g/kWh while  $\text{NO}_x$  is approximately 9.7 g/kWh. After taking  $\text{NO}_x$  emission into consideration, SFC increases and varies from 210 to 225 g/kWh, as can be seen from Figure 7. Besides,  $\text{NO}_x$  emission varies from 6.25 to slightly over 9.5 g/kWh, which is roughly within the  $\text{NO}_x$  limit range of Tier II (global) [13], whose lower limit is slightly over 10 g/kWh depending on engine speed. The Figure 7 shows a pareto front which consists of non-dominating result datasets. All the marked points in the pareto front are optimal candidates considering different weight placed on reduction of  $\text{NO}_x$  emission and a decrease of SFC. For example, when only considering to minimize the  $\text{NO}_x$  emission, it will lead to SFC of 225 g/kWh and  $\text{NO}_x$  emission of 6.25 g/kWh; when considering minimize SFC, it gives fuel consumption of around 210 g/kWh and  $\text{NO}_x$  emission of 9.7 g/kWh. Therefore, improvement of one objective function will accompany the deterioration of the other. Besides, it can be noticed that  $\text{NO}_x$  emission decreases rapidly when SFC increases from 213 g/kWh to 215 g/kWh, after which the compromise on specific fuel consumption is required to be much larger to achieve the same amount of  $\text{NO}_x$  reduction. Therefore, it may be very beneficial to choose the turning point around (214 g/kWh, 7.75 g/kWh) as an operational point, as fuel consumption does not compromise much to achieve the low  $\text{NO}_x$  emission. Smaller specific fuel consumption range appears in results at 20% load compared to 10% load, which ranges from 211.3 g/kWh to slightly higher than 212.8 g/kWh. Similarly, smaller range of  $\text{NO}_x$  emission occurs in this case than 10% load, resulting in approximately 8.5 to 8.9 g/kWh. Unlike Figure 7, there is not many turning points in Figure 8. In other words, the deterioration of the  $\text{NO}_x$  emission for improving specific fuel consumption is very similar through the whole range. Therefore, it will be more difficult to choose an optimal point if there is no clear idea about how to distribute weight on the two optimization objectives.

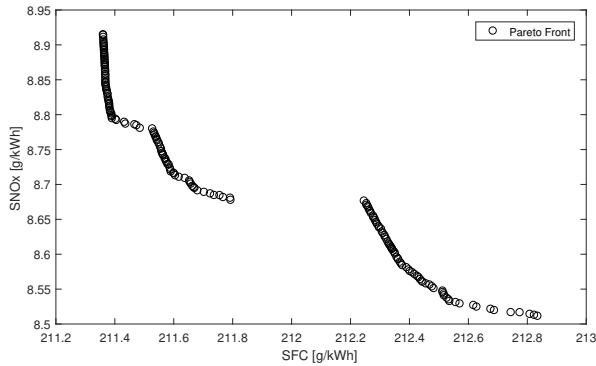


**FIGURE 8.** MULTI-OBJECTIVE OPTIMIZATION RESULT AT 20% MCR

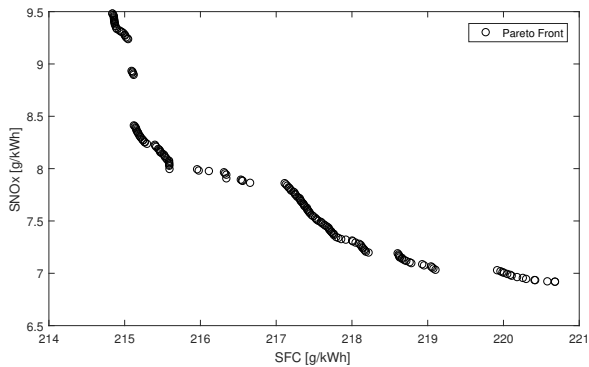


**FIGURE 9.** MULTI-OBJECTIVE OPTIMIZATION RESULT AT 50% MCR

When the power plant operates to deliver 50% of the maximum load, it conducts higher specific fuel consumption (seen in Figure 9). To achieve the minimum SFC, which is 214.8 g/kWh in this case, the  $\text{NO}_x$  emission will be 9.5 g/kWh. On the other hand, the fuel consumption will be around 220.8 g/kWh in order to achieve the minimum  $\text{NO}_x$  emission, which is around 7 g/kWh. The  $\text{NO}_x$  emission is also within the limit of Tier II.

### Optimization of Total Fuel Consumption with ESS

One promising alternative to reduce fuel consumption and emissions is to use the newest technologies in ESS, which is a device that stores energy and is able to consume and deliver power on demand. Hybridization of ESS in marine systems has many usages, which were summed up and described in [5].

In this part, optimization is undertaken to estimate optimal specific fuel consumption at steady-state power demand with charging and discharging an ESS. The ESS is considered in

**TABLE 5.** COMPARISON OF RESULTS FOR CONFIGURATION 1 WITHOUT AND WITH ESS (INDEX 1 INDICATES THE RESULTS WITHOUT ESS, AND INDEX 2 INDICATES THE RESULTS WITH ESS.)

Load	FC1	FC2	SFC1	SFC2	Number1	Number2
3%	82.8	162.3	230	213.7	1	1
6%	170.4	230	237	206.1	1	1
10%	253.4	318	211.2	198.7	1	1
15%	382.3	425.6	213	193.47	1	1
20%	490	526	205	188	1	1
30%	706	726.4	196	182	1	1
40%	901	861.9	188	180	1	1
50%	1122	1096	187	182.8	2	2
60%	1327	1320	184	183	2	2
70%	1535	1530	183	182	2	2
80%	1748	1734	182	180	2	2
90%	1954	1948	182	182	2	2

all three configurations. The ESS maximum charge/discharge power is assumed to be 400 kW, which means that the prime mover can deliver power at more flexible range. It should be noted that in real operation state of charge of the ESS has to be taken into account, so that charging or discharging can only be done for a limited period. Besides, the optimization objective is modified to be the specific fuel consumption.

It is clear from Table 5 that FC1 and FC2 at different loads are different due to the battery charging/discharging. Besides, the improvements are large at low loads when it comes to SFC, among which the highest reduction of specific fuel consumption is 30.9 g/kWh, or around 13%. Fuel saving potential is low at the high load due to high fuel economy before the ESS was connected.

From Table 6, it can be seen that the specific fuel consumption decreases and achieves an optimum when fewer engines are running. When the engines are running at low load, it is very beneficial to integrate an ESS as spinning reserve, as the load per genset is increased and thus leading to better fuel efficiency and less emission. At high loads such as 80% and 90% MCR, the fuel consumption is slightly higher when gensets operate together with ESS, where the ESS mode is strategic loading; and at low loads, it is the opposite.

In configuration 3, more engines can be stopped at conditions where there is low fuel efficiency. It can be observed in Table 7 that 6 engines stopped at 60% MCR load to achieve the optimal SFC with the assistance of ESS, which results in a potential SFC decrease of 5 g/kWh. Besides, by analyzing the engine number, one can tell that the configuration with low-power engines is very flexible and there exists frequent start and stop of the gensets. This is an advantage in terms of achieving better



**TABLE 6.** COMPARISON OF RESULTS FOR CONFIGURATION 2 WITHOUT AND WITH ESS (INDEX 1 INDICATES THE RESULTS WITHOUT ESS, AND INDEX 2 INDICATES THE RESULTS WITH ESS.)

Load	FC1	FC2	SFC1	SFC2	Number1	Number2
3%	71.8	141.7	199	186.4	1	1
6%	135	202	187	180.4	1	1
10%	214.2	218	180	180	1	1
15%	329	396	182.5	180.6	2	2
20%	442	430	184	180	3	2
30%	658	648	183	180	4	3
40%	876	857	182.5	180	5	4
50%	1101	1093	183.5	180	7	5
60%	1318	1292	183	180	8	6
70%	1522	1512	181	180	8	7
80%	1732	1728	180	180	8	8
90%	1954	1944	181	180	8	8

**TABLE 7.** COMPARISON OF RESULTS FOR CONFIGURATION 3 WITHOUT AND WITH ESS (INDEX 1 INDICATES THE RESULTS WITHOUT ESS, AND INDEX 2 INDICATES THE RESULTS WITH ESS.)

Load	FC1	FC2	SFC1	SFC2	Number1	Number2
3%	74	57	208	205	2	1
6%	153	152.4	213	205.7	3	3
10%	250	152.4	208	205.7	4	3
15%	381	368	211.7	205.4	7	6
20%	506	489	210	205	8	7
30%	761	734	211	205	13	10
40%	1015	980	211	205	17	13
50%	1260	1228	210	205	22	18
60%	1512	1474	210	205	27	21
70%	1739	1721	207	205	28	25
80%	1987	1965	207	205	29	28
90%	2225	2214	206	205	29	29

fuel economy. However, it requires a better power management system to govern and control the gensets and avoiding stops and starts that give insignificant fuel saving.

## CONCLUSION

The simulation results shows that by integrating ESS in the power plant configurations, allowed gensets to run at more optimal specific fuel consumption, especially in configuration 2 and 3 where there are a higher number of gensets available in the

power system than without integrating ESS in the system. The optimization based on a genetic algorithm to find an optimal operating point for gensets under different power demands for an offshore construction vessel has been explored for three different power system configuration. Single and multi-objective optimization with regard to minimizing fuel consumption and NO<sub>x</sub> emission has been carried out and the results are compared for the power plant with and without energy storage systems.

## REFERENCES

- [1] Ådnanes, A. K., 2003. "Maritime electrical installations and diesel electric propulsion". *ABB AS Norway*.
- [2] Thorat, L., and Skjetne, R., 2017. "Load-dependent start-stop of gensets modeled as a hybrid dynamical system". *IFAC-PapersOnLine*, **50**(1), pp. 9321–9328.
- [3] Dieselnets, 2017. Emission Standards: International: IMO Marine Engine Regulations. Retrieved from <https://www.dieselnets.com/standards/inter/imo.php>.
- [4] DNV-GL, 2011. Newbuildings Special Equipment and Systems Dynamic Positioning Systems.
- [5] Lindtjørn, J. O., Wendt, F., and Gundersen, B., 2014. "Demonstrating the benefits of advanced power systems and energy storage for DP vessels". *In Proc. DP Conf., Houston, TX, USA*.
- [6] Miyazaki, M. R., and Sørensen, A. J., 2016. "Reduction of fuel consumption on hybrid marine power plants by strategic loading with energy storage devices". *IEEE Power and Energy Technology Systems Journal*, **3**(4), pp. 207–217.
- [7] Iverson, J., 2017. "How to size a genset: Proper generator set sizing requires analysis of parameters and loads". *Cummins Power Generation - Available online*.
- [8] Reeves, C. R., 1995. "A genetic algorithm for flowshop sequencing". *Computers and Operations Research*, **22**(1), pp. 5–13.
- [9] Perkins. The Perkins 2506C-E15TAG Electric power engine. Available online.
- [10] Rolls-Royce. The Rolls-Royce Bergen B32:40V generating set. Available online.
- [11] Osen, O. L., 2016. "Optimizing electric energy production on-board offshore vessels: Vessel power consumption profile and production strategies using genetic algorithms". In *OCEANS 2016 - Shanghai, IEEE*, pp. 1–10.
- [12] ElectronicDesign, 2017. Understand Efficiency Ratings Before Choosing An AC-DC Supply.
- [13] MARPOL, 2017. Annex VI - Regulation 13 - Nitrogen oxides (NO<sub>x</sub>).

## Appendix A: Single Line Diagram of Configurations

Proposed system configurations are illustrated as single line diagrams in Figures 10, 11, and 12.

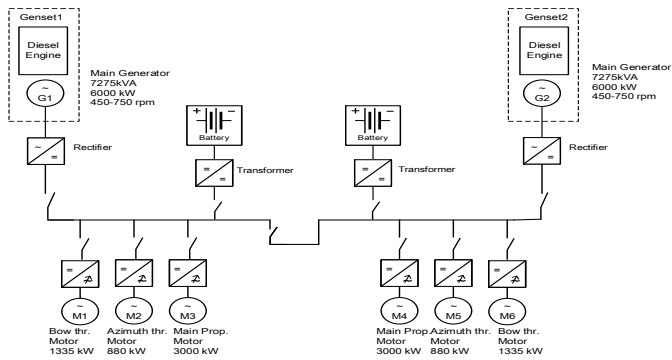


FIGURE 10. Configuration 1

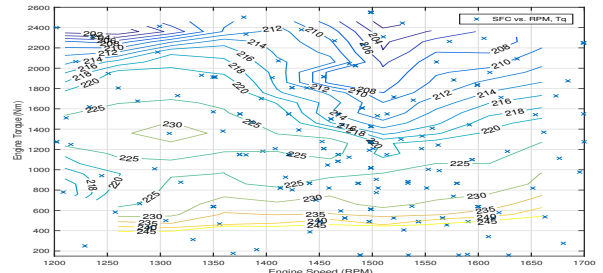


FIGURE 13. SFC map of Perkins 2506C.

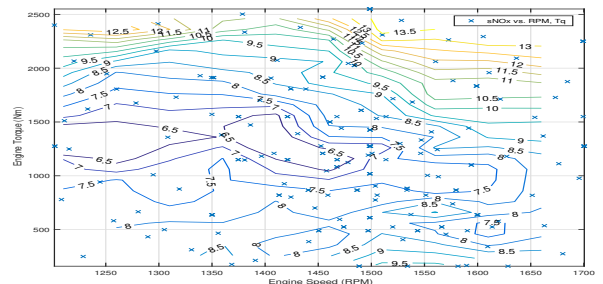


FIGURE 14. SNO<sub>x</sub> map of Perkins 2506C.

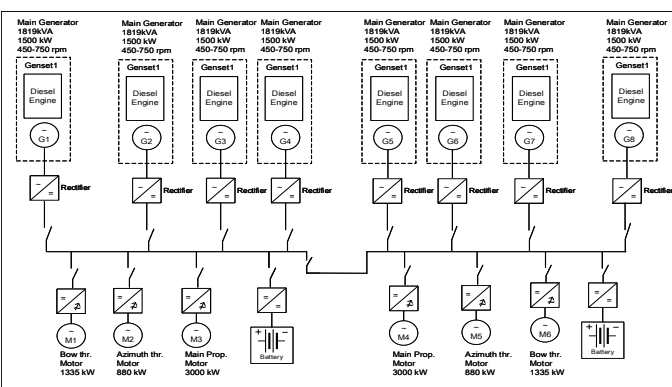


FIGURE 11. Configuration 2

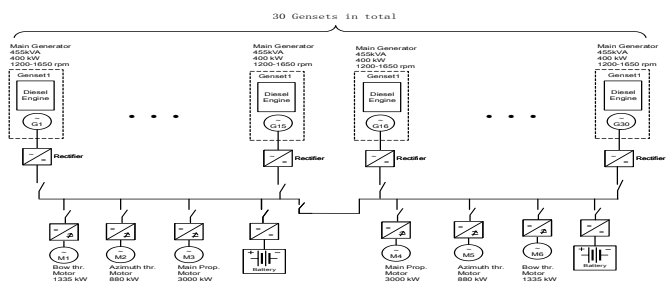


FIGURE 12. Configuration 3

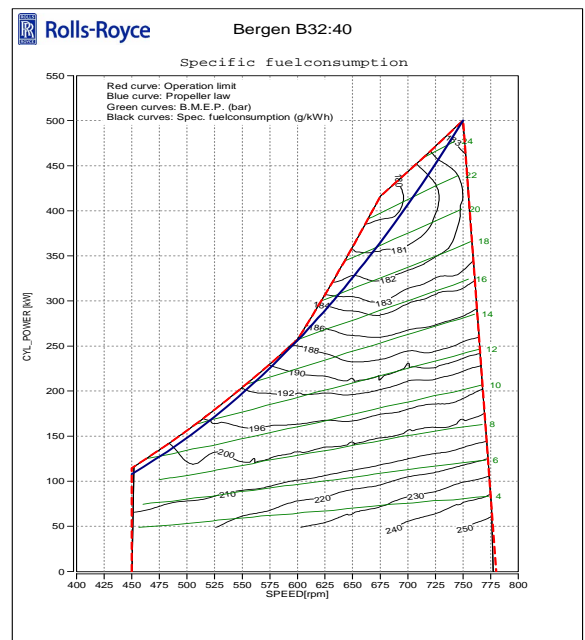


FIGURE 15. SFC map of Rolls Royce Bergen B32:40. Source: [11].

## Appendix B: Engine Specific Fuel Map

Figures 13 and 14 depicts the SFC and SNO<sub>x</sub> curve of Perkins 2506C against engine power and speed. Figure 15 shows the SFC curve of Rolls Royce Bergen B32:40 against cylinder power and speed.